

PHASE SPACE MANIPULATIONS IN MODERN ACCELERATORS*

Dao Xiang[†], Shanghai Jiao Tong University, Shanghai, China

Abstract

Beam manipulation is a process to rearrange beam's distribution in 6-D phase space. In many cases, a simple phase space manipulation may lead to significant enhancement in the performance of accelerator based facilities. In this paper, I will discuss various beam manipulation techniques for tailoring beam distribution in modern accelerators to meet the requirements of various applications. These techniques become a new focus of accelerator physics R&D and hold great promise in opening up new opportunities in accelerator based scientific facilities.

INTRODUCTION

The ability to tailor a beam's 6-D phase space to meet the demands of various applications is of fundamental interest in accelerator physics. For instance, the electron bunch length typically needs to be reduced in FELs to drive the exponential growth process while it may need to be increased in storage rings to increase beam life time. Beam manipulations include a wide array of techniques that use rf cavities, dispersive elements, lasers, etc. to rearrange beam distribution in 6-D phase spaces. On the one hand, one has the freedom to use many elements to design a beam for a specific application (see. e.g. [1]); on the other hand, beam manipulation has to obey some basic rules (e.g. the emittances of the subspaces cannot be partially transferred from one plane to another if the beam is uncoupled before and after the transformation [2]). Here I will discuss a few representative beam manipulation techniques and show how they may enhance the capabilities of modern accelerators.

GENERAL DISCUSSIONS

In transverse plane, dipoles are used to bend the beam and quadrupoles are used to focus the beam. When they are integrated in a suitable way, they can form a closed loop (an electron storage ring) which allows the beam to circulate for millions of thousands turns. While it appears trivial to control the transverse beam size with quadrupoles, focusing the beam to extremely small size requires special efforts. For instance, a ~ 500 m final focus beam line is needed to focus the electron beam to nanometer (nm) level in linear colliders [3]; another extreme is electron microscope where the spherical aberration is corrected up to the 5th order to provide sub-50 pm resolution which allows one to see individual Hydrogen atom [4].

In longitudinal plane, beam phase space manipulation typically requires an element to change beam energy and a dispersive element to change beam path length. This is be-

cause relativistic electrons travel more or less with the speed of light (e.g., for 1 GeV electron, $1 - v/c \approx 1.3 \cdot 10^{-7}$). As a result, for modern beams with typical small energy spreads, the relative longitudinal velocities of electrons are so small that they do not change their relative positions when the beam travels along a straight line in a drift. With a dispersive element, one can force the particles to follow different paths and the beam longitudinal distribution can be readily shaped.

BEAM MANIPULATION FOR FELS

So far most of the high-gain FELs in the short wavelength (VUV to hard x-ray regime) have operated in the SASE mode in which radiation from the electron beam shot noise is exponentially amplified to the GW level. While a SASE FEL has excellent transverse coherence, its temporal coherence is rather limited (noisy in temporal profile and spectrum). In this section we discuss several beam manipulation techniques that may improve temporal coherence of FELs by providing coherent bunching to seed the FEL amplification process.

To provide bunching at short wavelength, fine structures in beam current distribution have to be created. The creation of a charge density modulation at sub-optical wavelengths in an electron beam with lasers is analogous to the manipulation of the electron bunch length in a magnetic bunch compressor. The difference is that the energy chirp (correlation between a particle's energy and its longitudinal position) is imprinted by lasers rather than RF cavities. The process of longitudinal bunch compression, to the first order, can be described as a linear transformation where the bunch length is reduced while the energy spread (conservation of phase space area) and peak current (conservation of charge) are both increased. This is achieved by first accelerating the beam off-crest in RF cavities to establish a correlated energy chirp (e.g. with bunch head having a slightly lower energy than the bunch tail), and then sending the beam through a dispersive chicane. The particles with lower energy are bent more in the chicane and therefore tra-

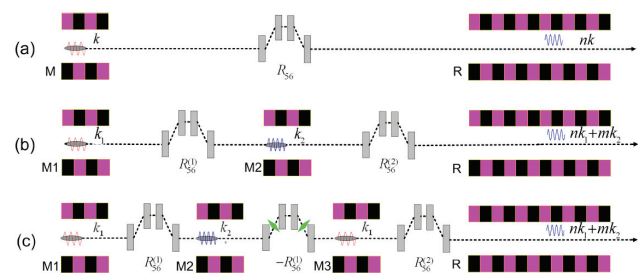


Figure 1: Various harmonic generation schemes for seeding FELs.

* Work supported by the National Natural Science Foundation of China under Grants No. 11327902.

[†] dxiang@sjtu.edu.cn

verse a longer path length than the higher energy particles that are bent less. As a result, the low energy electrons slip back longitudinally while the high energy electrons catch up, which leads to bunch compression.

Replacing the RF cavity with a laser allows one to create much finer structures in beam phase space without changing the overall bunch length. This is because the laser wavelength is typically much shorter than the electron beam duration, so the laser does not give beam a net energy chirp. As a result, after dispersion the overall bunch duration is kept constant. Instead, the time-varying laser field imprints a sinusoidal energy chirp (called an energy modulation) on the beam phase space which leads to varying local compression/decompression of the beam current on the scale of the laser wavelength after dispersion. The result is a density modulation in the current distribution of the beam, both at the laser frequency and at its harmonics.

For example, the phase space evolution in high-gain harmonic generation (HG HG [5]) scheme (Fig. 1a) is shown in Fig. 2. A laser is first used to interact with the beam in a modulator to produce sinusoidal energy modulation in beam phase space (Fig. 2b). After passing through a chicane, half of the particles that have the negative energy chirp (blue particles in Fig. 2b and Fig. 2c) are compressed, while the other half with the positive energy chirp (red particles in Fig. 2b and Fig. 2c) are decompressed. As a result of this transformation, the energy modulation is effectively converted into a density modulation (see Fig. 2d where the beam density consists of many spikes equally separated by the laser wavelength) that contains harmonic frequency components of the laser fundamental frequency.

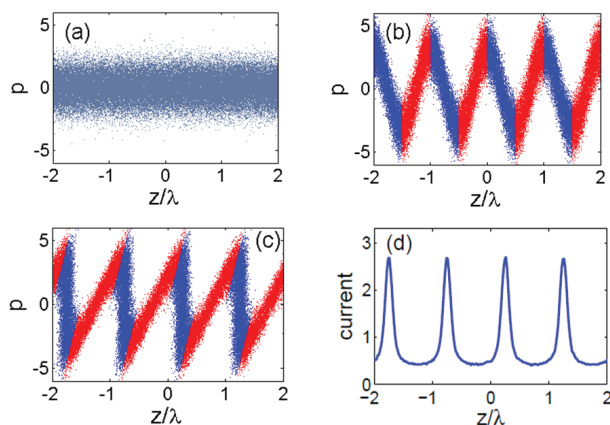


Figure 2: Evolution of the phase space in HG HG scheme. (a) before the modulator; (b) after the modulator; (c) after the chicane; (d) density distribution after the chicane normalized to the initial beam current. The horizontal axis is the beam longitudinal position normalized to the laser wavelength and the vertical axis is particle's energy deviation with respect to the reference particle normalized to the rms slice energy spread of the beam. The energy modulation is three times larger than the beam energy spread.

Analysis shows that the width of the current spike normalized to the laser wavelength is approximately $1/A$, where $A = \Delta E/\sigma_E$ is the ratio of energy modulation amplitude ΔE to the beam energy spread σ_E . Therefore, in general generation of the h th harmonic requires the energy modulation to be approximately h times larger than beam energy spread, an undesired consequence for FEL applications where the increased energy spread may significantly reduce the FEL gain. Another undesired consequence for HG HG is that if the h th harmonic is to be achieved, the peak current of the bump is also increased by about h times (as can be seen in Fig. 1d), which may cause undesirable collective effects. Furthermore, the spectrum of the bunching is found to be sensitive to beam imperfections such as nonlinear beam energy chirps that may easily broaden the bunching spectrum by changing the separation of the current spikes [6, 7].

These limitations can be overcome with the echo-enabled harmonic generation (EEHG [8, 9]) scheme in the double modulator-chicane system (Fig. 1b). In EEHG the beam is also first energy modulated by a laser in the first modulator. But quite differently, the first chicane is chosen to have a large momentum compaction such that after passing through the strong chicane the density modulation is macroscopically smeared (Fig. 3a). Simultaneously, complicated fine structures (e.g. 'energy banding') are introduced into the phase space, which has been recently observed experimentally [10]. A second laser is then used to further modulate the beam energy in the second modulator (Fig. 3b) to imprint additional correlations in phase space. A second weaker chicane orients these correlations vertically in the energy space, which yields a charge density modulation at very high harmonic frequencies. As a result of this nonlinear process, the harmonic bunching structure emerges as a re-coherence effect after a short disappearance, like an echo

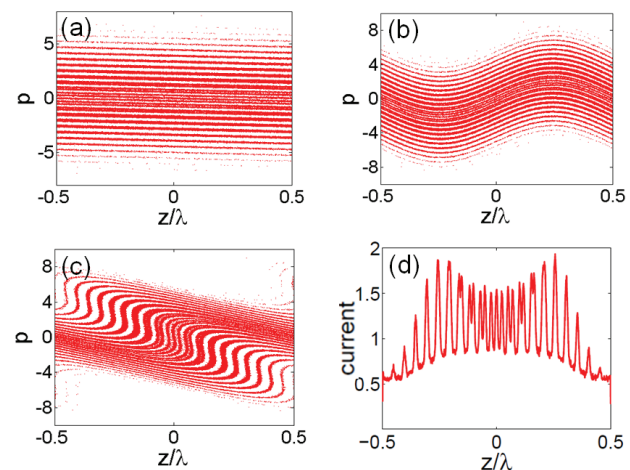


Figure 3: Evolution of the longitudinal phase space in EEHG scheme. (a) after the first strong chicane; (b) after the second modulator; (c) after the second weak chicane; (d) density distribution after the second chicane.

(Fig. 3c and Fig. 3d). The first stage of EEHG may also be understood as bunch local decompression such that the spread of each energy band is reduced compared to the initial energy spread; and the second stage of EEHG is then similar to HGHG.

The key advantage of EEHG technique is that it can generate very high harmonics with harmonic number much larger than the ratio of energy modulation to energy spread. This makes it possible to generate very high frequency bunching while simultaneously keeping the beam energy spread small, which allows the generation of soft x-rays from a UV seed laser in a single stage. Another advantage of EEHG is that by splitting the single current bump into many bumps per wavelength, the peak current of each current bump can be significantly reduced, which mitigates the potential collective effects related to the high peak current. For instance, as seen in Fig. 3d, with the energy modulation three times larger than the beam energy spread, the peak current is only increased by a factor of 2 while the harmonic number is extended to ~ 20 . Even higher harmonics can be produced by increasing the momentum compaction of the first chicane while keeping the energy modulation amplitudes essentially unchanged. Furthermore, due to the highly nonlinear phase space gymnastics that decompress local regions of the beam, the spectrum of the bunching is made to almost immune to the phase space imperfections. This allows the generation of transform-limited highly coherent radiation in realistic conditions when the beam has considerable nonlinear chirps [11].

To push the harmonic number to beyond 100, very recently a novel seeding scheme that uses a triple modulator-chicane (TMC) system has also been proposed [12]. This scheme is schematically shown in Fig. 1c where the first and second chicanes have opposite momentum compaction and the first and third lasers have the same wavelength and π phase shift. To illustrate the physics behind the TMC scheme, the evolution of the beam longitudinal phase space is shown in Fig. 4. For simplicity, in Fig. 4 the lasers have the same wavelength in the three modulators and only the phase space within one wavelength region is shown.

The beam phase space after interaction with the first laser is shown in Fig. 4a where the energy modulation is 3 times larger than the beam slice energy spread. Similar to the EEHG scheme, separated energy beamlets are generated (Fig. 4b) after the beam passes through the first chicane with a moderate R_{56} as a result of bunch decompression with a decompression factor D . After interaction with the second laser of which the energy modulation is 20 times smaller than beam slice energy spread, the beam phase space evolves to that in Fig. 4c. Because the energy modulation is much smaller than beam's initial energy spread, it is actually very difficult to see the difference between Fig. 4b and Fig. 4c. The second chicane with opposite momentum compaction ($R_{56}^{(2)} = -R_{56}^{(1)}$) compresses the beamlets by a factor of D and amplifies the modulation imprinted in M2. The resulting beam phase space is shown in Fig. 4d which is similar to that in Fig. 4a. If no modulation is imposed

in M2, the second chicane will restore beam phase space to the same distribution as that before the first chicane, because the transfer matrix from the exit of M1 to the exit of the second chicane is unity. With a small energy modulation in M2, the second chicane will transform the beam phase space to a distribution similar to that before the first chicane with the presence of energy modulation from M2 superimposed on the modulation from M1 (Fig. 4d).

The laser in M3 is chosen to give the beam the same modulation amplitude as that in M1, but with π phase shift, so that the overall energy modulation in M1 is canceled in M3. After the cancellation, the modulation from M2 becomes dominant, as shown in Fig. 4e. The wavelength of the modulation in Fig. 4e is roughly D times shorter than that in M2. A third chicane with small R_{56} further converts the energy modulation into density modulation (Fig. 4f). By integrating the modulators and chicanes in a clever way, the 22nd harmonic is generated with a modulation in M2 that is 20 times smaller than beam slice energy spread and the final energy spread growth is only about 15%.

The unique advantages of TMC scheme that only a small energy modulation is needed in M2 and the second chicane compresses the modulation imprinted in M2 to shorter wavelength opens new opportunities for using low power high-order harmonic generation (HHG) source (see, for example [13]) at short wavelength to seed x-ray FELs. As an example, in [12] the feasibility of generating significant bunching at 1 nm and below from a low power (100 kW) HHG seed at 20 nm assisted by two moderate power UV lasers at 200 nm while keeping the energy spread growth within 40% has been shown. The supreme up-frequency conversion efficiency of the TMC scheme together with its unique advantage in maintaining beam energy spread opens new opportunities for generating fully coherent x-rays at sub-nanometer wavelength from external seeds.

Both HGHG and EEHG have been demonstrated experimentally. So far the record for HGHG is the 60th harmonic obtained in a two-stage configuration [14] and that

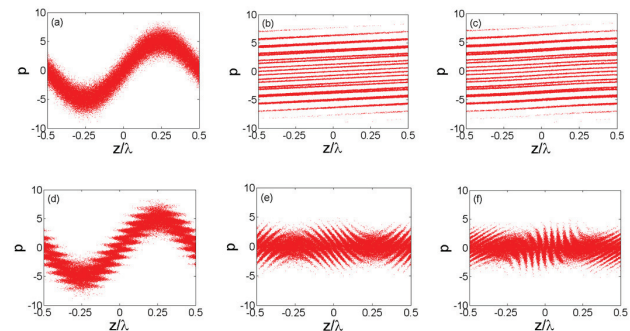


Figure 4: Evolution of the longitudinal phase space in TMC scheme. (a)-After the first modulator; (b)-After the first chicane; (c)-After the second modulator; (d)-After the second chicane; (e)-After the third modulator; (f)-After the third chicane.

for EEHG in a single stage is 15th harmonic [15]. While the EEHG is still in the early experimental development stage [15–18], the two distinct advantages of EEHG, i.e. high frequency up-conversion efficiency and insensitivity to electron beam phase space imperfections have both been demonstrated. For instance, Fig. 5 shows the radiation spectra of HGHG and EEHG produced with a 2.4 micron seed laser when the beam has considerable quadratic energy chirp. The beam is accelerated at an off-crest phase (about 2.5 degrees from on-crest phase) to imprint a positive energy chirp and the exact energy chirp is varying from the fluctuation of timing jitter and RF phase jitter. From the results, one can see that while the radiation from HGHG has large fluctuations in the central wavelength and relatively large bandwidth, that from EEHG is essentially unchanged with a much narrower bandwidth. These results should forward the development of future seeded x-ray FELs that aim to produce laser-like x-rays.

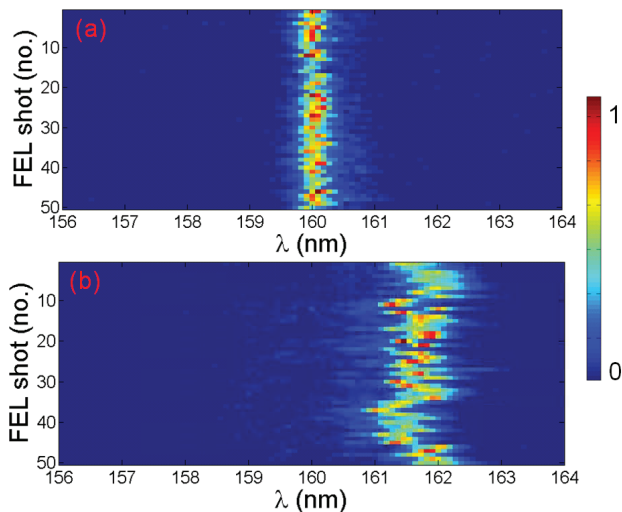


Figure 5: Fifty consecutive radiation spectra for EEHG (a) and HGHG (b) with a chirped beam. Note, the central wavelength of HGHG signal is shifted by the linear chirp and the bandwidth of the HGHG signal is increased by the nonlinear chirp, while those for EEHG are essentially unaffected.

BEAM MANIPULATION FOR THZ RADIATION

For structures at THz wavelength and above, the drive laser as required in a photocathode rf gun may be shaped accordingly to generate the desired pattern in beam current distribution, taking advantage of the promptness of the photoemission process [19–21]. Alternatively, one may use two lasers to manipulate the beam longitudinal phase space for generation of charge density modulation at THz frequency. For instance, in the scheme proposed in [22] a laser is used to generate energy modulation in the beam phase space in the first undulator; after interacting with the second laser, the beam phase space consists of fast modulation at the

sum frequency and a slow modulation at the difference frequency (see Fig. 6). After passing through a chicane, the energy modulation at the difference frequency can be converted to density modulation. If the frequencies of the two lasers are close to each other, the difference frequency will be much lower than the laser frequency. In this case the relativistic electron beam is used as the nonlinear medium to down-convert the frequency of two optical lasers to THz range, and therefore one can generate long-scale periodic structures in electron beam through short-scale laser modulations.

This technique has been demonstrated at SLAC’s NLCTA where density modulation around 10 THz was generated by down-converting the frequencies of an 800 nm laser and a 1550 nm laser [23]. One of the many advantages of this technique is the flexibility it offers to tune the central frequency of the modulation, which can be achieved through tuning of laser wavelengths, beam energy chirp, and chicane momentum compaction. In principle, this allows one to generate coherent narrow-band THz radiation covering the whole THz range. A variant of this scheme that allows one to use two lasers with the same wavelength to produce THz using the EEHG setup has also been briefly discussed in [23] and studied in detail in [24]. Here an energy chirp is used to produce a slight shift of the wavelength of the modulation from the first laser, which also leads to density modulation at THz frequency when superimposed with the second laser modulation. This scheme removes the need of an OPA for producing lasers with different wavelengths for THz generation.

It is also possible to use a transverse mask to generate fine structures in beam transverse distribution, and then use emittance exchange technique [25–27] to convert the spatial structures into time structures [28]. For a beam line that couples the beam dynamics in x and z planes, analysis shows if its 4 by 4 transfer matrix has such a form that it is 2 by 2-block antidiagonal, then a particle’s final transverse

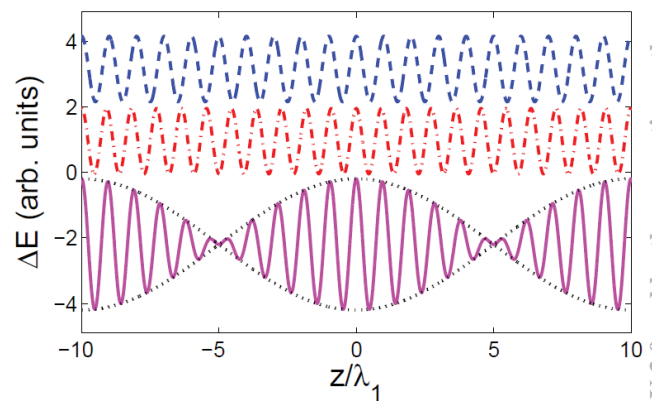


Figure 6: Energy modulation with a laser at λ_1 (blue line) and at $0.9\lambda_1$ (red line); a combination of the two energy modulations (magenta line); the black dotted line illustrates the envelope of the slow modulation at the difference frequency of the two lasers.

coordinates will only depend on its initial longitudinal coordinates, and vice versa. As a result, beam's transverse and longitudinal degrees of freedom will be exchanged after the beam passes through the beam line. The first beam line for transverse-to-longitudinal EEX proposed in 2002 consists of a RF deflecting cavity in the center of a chicane [25]. This scheme is easy to implement, but the exchange is not complete. Later a complete EEX beam line was found in which the deflecting cavity is put between two identical doglegs [26]. However, this scheme introduces offset in beam trajectory which might be undesirable in some cases. Recently a chicane type exact EEX beam line was also proposed [27] where a pair of quadrupoles is used to form a negative unity transfer matrix for the transverse plane in the chicane. The negative unity section reverses the dispersion of the first half of the chicane, which is optically equivalent to flipping the sign of a dogleg. This beam line also provides exact EEX and may be easier to implement because it doesn't introduce offset, and turning off the quadrupoles and deflecting cavity makes the beam line a simple chicane. Because the transverse and longitudinal phase space are exchanged, one can produce tailored beam distribution in longitudinal plane by shaping the initial beam distribution in transverse plane [28].

BEAM MANIPULATION FOR ADVANCED ACCELERATORS

Advanced accelerators driven by laser and electron beam hold great promise in downsizing accelerator based scientific facilities through the orders of magnitude higher acceleration gradient. With a special mask, one may generate a beam with linearly ramped current [29] through emittance exchange that will significantly increase the transformer ratio in electron beam driven advanced accelerators.

Here I will focus on how one may enhance the performance of inverse FEL (IFEL) where a high power laser is used to boost beam energy in an undulator. In rf accelerators, the electron bunch is much shorter than the wavelength of the rf field, and therefore a monoenergetic beam can be routinely obtained. However, obtaining a monoenergetic beam in laser accelerators is not trivial, because typically the electron bunch length is much longer than laser wavelength and different particles would see different phases (some get accelerated while others are decelerated). One promising way to obtain monoenergetic beams in laser accelerators is to first use a laser to generate microbunches, and then put the bumps at the acceleration phase so that most of the particles see more or less the same field which will lead to net acceleration. This has been demonstrated both at FIR wavelength [30] and optical wavelength [31].

As shown in Fig. 7, with the electron bunch being much longer than laser wavelength, in a single stage IFEL half of the electrons are accelerated while the other half decelerated (middle). In a cascaded IFEL, much more electrons can be accelerated by a strong laser pulse after being packed into optical microbunches by a weaker initial laser pulse

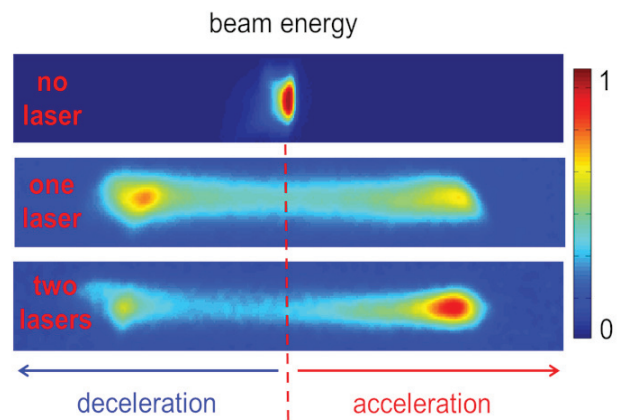


Figure 7: Benefits of cascading in an optical IFEL: a relativistic electron beam with small energy spread (top) can be accelerated with a co-propagating laser (middle), or with two lasers in sequence (bottom).

(bottom), which leads to reduced beam energy spread and higher trap efficiency.

BEAM MANIPULATION FOR UED/UEM

Accelerator based ultrafast electron diffraction (UED [32–34]) and ultrafast electron microscopy (UEM [35–37]) facilities are complementary to FELs and may also provide both high temporal and spatial resolution in probing matter at extremely high precision. In UEDs, one of the main challenges is how to produce beam with ~ 10 fs duration and sufficient number of electrons (say $\sim 10^6$). The beam at the exit of the photocathode rf gun typically has a positive energy chirp from the longitudinal space charge force, which would further increase bunch length in the following drift. One solution is to use an rf cavity to reverse the energy chirp and then the bunch length may be reduced in a drift or chicane. The other is to use an Alpha magnet that has positive R_{56} to compress the beam. With these manipulation in longitudinal plane, one may realize ~ 10 fs resolution in UED.

In UEMs, one of the main challenges is to produce beam with energy spread below 10^{-4} and normalized emittance below 0.1 micron [36, 37]. To reduce beam emittance, the beam charge needs to be reduced and bunch length needs to be increased to mitigate the space charge effect. However, as bunch length increases, the nonlinear rf curvature tends to increase the beam global energy spread. This can be compensated for with a harmonic cavity, similar to that in FELs where harmonic cavities are used to linearize the beam longitudinal phase space to enhance the performance of bunch compressors. For instance, as shown in Fig. 8, with the compensation in the harmonic cavity, beam energy spread can be reduced from 10^{-3} to below 10^{-4} .

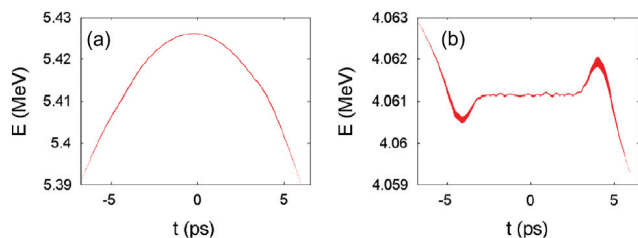


Figure 8: Beam longitudinal phase space at the exit of the s-band photocathode rf gun (a) and at the exit of the c-band harmonic cavity (b).

SUMMARY

In this paper, various techniques for manipulating beam distribution in phase space are discussed. I focused on the techniques that I'm most familiar with. There are many techniques not included in the discussion, such as beam conditioning, emittance partitioning, etc., and the interested readers can find more information elsewhere. For readers particularly interested in beam manipulation with lasers, more information can be found in the review article [1]. These techniques become a new focus of accelerator physics R&D and I believe very likely these advanced concepts will open up new opportunities in accelerator based scientific facilities and the science enabled by them.

ACKNOWLEDGMENT

I want to thank my SLAC colleagues: A. Chao, G. Stupakov, T. Raubenheimer, K. Bane, Y. Cai, Y. Ding, M. Dunning, P. Emma, W. Fawley, C. Hast, E. Hemsing, X. Huang, Z. Huang, A. Marinelli, C. Pellegrini, F. Wang, J. Wang, S. Weathersby, J. Wu etc. for many useful collaborations and discussions. I am also grateful to M. Couprie, C. Behrens, H. Deng, C. Feng, P. Musumeci, G. Penn, S. Reiche, W. Wan, D. Wang, Z. Zhao, A. Zholents, etc. for useful international collaborations and discussions. I want to thank the support from DOE Early Career Award from 2012 to 2014.

REFERENCES

[1] E. Hemsing, G. Stupakov, D. Xiang and A. Zholents, *Rev. Mod. Phys.* 86, 897 (2014).
 [2] E. Courant, *Conservation of phase space in Hamiltonian systems and particle beams*, in *Perspectives in Modern Physics, Essays in Honor of Hans A. Bethe*, edited by R. E. Marshak (Interscience Publishers, New York), p. 257.
 [3] P. Raimondi and A. Seryi, *Phys. Rev. Lett.* 86, 3779 (2001).
 [4] R. Erni *et al.*, *Phys. Rev. Lett.* 102, 096101 (2009).
 [5] L.-H. Yu, *Phys. Rev. A* 44, 5178 (1991).
 [6] T. Shaftan and L.-H. Yu, *Phys. Rev. E* 71, 046501 (2005).
 [7] A. Marinelli, C. Pellegrini, L. Giannessi and S. Reiche, *Phys. Rev. ST Accel. Beams* 13, 070701 (2010).
 [8] G. Stupakov, *Phys. Rev. Lett.* 102, 074801 (2009).
 [9] D. Xiang and G. Stupakov, *Phys. Rev. ST Accel. Beams* 12, 030702 (2009).

[10] E. Hemsing *et al.*, *Phys. Rev. ST Accel. Beams* 17, 010703 (2014).
 [11] Z. Huang *et al.*, in *Proceedings of FEL 09* (Liverpool, 2009), p.127.
 [12] D. Xiang and G. Stupakov, *New J. Phys.* 13, 093028 (2011).
 [13] T. Popmintchev *et al.*, *Nature Photon.* 4, 822 (2010).
 [14] E. Allaria *et al.*, *Nature Photonics* 7, 913 (2013).
 [15] E. Hemsing *et al.*, *Phys. Rev. ST Accel. Beams* 17, 070702 (2014).
 [16] D. Xiang *et al.*, *Phys. Rev. Lett.* 105, 114801 (2010).
 [17] D. Xiang *et al.*, *Phys. Rev. Lett.* 108, 024802 (2012).
 [18] Z. Zhao *et al.*, *Nature Photon.* 6, 360 (2012).
 [19] J. Neumann *et al.*, *J. Appl. Phys.* 105, 053304 (2009).
 [20] P. Musumeci, R.K. Li and A. Marinelli, *Phys. Rev. Lett.* 106, 184801 (2011).
 [21] Y. Shen *et al.*, *Phys. Rev. Lett.* 107, 204801 (2011).
 [22] D. Xiang and G. Stupakov, *Phys. Rev. ST Accel. Beams* 12, 080701 (2009).
 [23] D. Dunning *et al.*, *Phys. Rev. Lett.* 109, 074801 (2012).
 [24] Z. Wang *et al.*, *Echo-enabled tunable terahertz radiation generation with a laser-modulated relativistic electron beam*, *Phys. Rev. ST Accel. Beams*, in press (2014).
 [25] M. Cornacchia and P. Emma, *Phys. Rev. ST Accel. Beams* 5, 084001 (2002).
 [26] P. Emma *et al.*, *Phys. Rev. ST Accel. Beams* 9, 100702 (2006).
 [27] D. Xiang and A. Chao, *Phys. Rev. ST Accel. Beams* 14, 114001 (2011).
 [28] Y.-E. Sun *et al.*, *Phys. Rev. Lett.* 105, 234801 (2010).
 [29] P. Piot *et al.*, *Phys. Rev. ST Accel. Beams* 14, 022801 (2011).
 [30] W. Kimura *et al.*, *Phys. Rev. Lett.* 86, 4041 (2001).
 [31] D. Dunning *et al.*, *Phys. Rev. Lett.* 110, 244801 (2013).
 [32] X. Wang, D. Xiang, T. Kim, and H. Ihee, *Potential of Femtosecond Electron Diffraction Using Near-Relativistic Electrons from a Photocathode RF Electron Gun*, *Journal of the Korean Physical Society*, 48, 390 (2006).
 [33] J. Hastings *et al.*, *Appl. Phys. Lett.* 89, 184109 (2006).
 [34] P. Musumeci *et al.*, *Appl. Phys. Lett.* 97, 063502 (2010).
 [35] J. Yang *et al.*, *Proc. of IPAC14*, p.2205 (2014).
 [36] D. Xiang *et al.*, *Nucl. Instrum. Methods Phys. Res., Sect. A* 759, 74 (2014).
 [37] R. Li and P. Musumeci, *Phys. Rev. Applied*, 2, 024003 (2014).